



CHALMERS

Chalmers Publication Library

A 200 GHz CVD Graphene FET Based Resistive Subharmonic Mixer

This document has been downloaded from Chalmers Publication Library (CPL). It is the author's version of a work that was accepted for publication in:

2016 IEEE MTT-S International Microwave Symposium, IMS 2016, San Francisco, 22-27 May 2016 (ISSN: 0149-645X)

Citation for the published paper:

Zhang, Y. ; Andersson, M. ; Stake, J. (2016) "A 200 GHz CVD Graphene FET Based Resistive Subharmonic Mixer". 2016 IEEE MTT-S International Microwave Symposium, IMS 2016, San Francisco, 22-27 May 2016 pp. 1-4.

<http://dx.doi.org/10.1109/MWSYM.2016.7540287>

Downloaded from: <http://publications.lib.chalmers.se/publication/237057>

Notice: Changes introduced as a result of publishing processes such as copy-editing and formatting may not be reflected in this document. For a definitive version of this work, please refer to the published source. Please note that access to the published version might require a subscription.

Chalmers Publication Library (CPL) offers the possibility of retrieving research publications produced at Chalmers University of Technology. It covers all types of publications: articles, dissertations, licentiate theses, masters theses, conference papers, reports etc. Since 2006 it is the official tool for Chalmers official publication statistics. To ensure that Chalmers research results are disseminated as widely as possible, an Open Access Policy has been adopted. The CPL service is administrated and maintained by Chalmers Library.

(article starts on next page)

A 200 GHz CVD Graphene FET Based Resistive Subharmonic Mixer

Yaxin Zhang, Michael A. Andersson, and Jan Stake

Terahertz and Millimetre Wave Laboratory, Chalmers University of Technology, Göteborg, Kemivägen 9, 412 96, Sweden

Abstract—We report on the design and characterization of a 200 GHz resistive subharmonic mixer based on a single, multi-channel CVD graphene field effect transistor (G-FET). The device has gate length $0.5 \mu\text{m}$ and width $2 \times 40 \mu\text{m}$. The integrated mixer circuit is implemented in coplanar waveguide (CPW) technology and realized on a $100 \mu\text{m}$ thick high resistive silicon substrate. The measured mixer conversion loss (CL) is $34 \pm 3 \text{ dB}$ across 190-210 GHz band with 10 dBm local oscillator (LO) pumping power and the overall minimum CL gives 31.5 dB at 190 GHz.

Index Terms—Graphene, FETs, subharmonic resistive mixers, millimeter wave integrated circuits, coplanar waveguide.

I. INTRODUCTION

Graphene, a two-dimensional monolayer of carbon atoms [1], currently draws great attention in nanotechnology research aiming at improved high frequency electronics. The high intrinsic carrier mobility as well as high carrier saturation velocity make it a promising candidate for high speed analog devices such as transistors operating in the millimeter wave and terahertz frequency bands [2]. Potential applications of such graphene based components and circuits are wireless high speed communication links [3], and security imaging [4].

However, with the exception of graphene millimeter wave [5], [6] and terahertz power detectors [7], [8], no graphene integrated circuits operating above 30 GHz [9], [10] have been demonstrated. To date, considerable efforts have been made to develop graphene field effect transistor (G-FET) based microwave devices [11], [12] and circuits with extensive focus on frequency translating devices. While fundamental single-ended [13] and double balanced [14] resistive mixers achieve conversion loss (CL) of 14 dB at 2 GHz and 33 dB at 3.6 GHz, the inherent symmetry of G-FET channel conductance was not utilized. For this purpose, subharmonic resistive G-FET mixers have been reported with 22 dB and 19 dB CL at 2-5 GHz and 24-31 GHz [10], [15], respectively. As can be seen, the operating frequency of the devices and circuits listed above are far below the anticipated values. Therefore, increasing the G-FET based integrated circuit operation frequency and performance are keys in order to satisfy the expectation of graphene.

In this paper, we demonstrate a subharmonic resistive mixer circuit operating at 190-210 GHz based on a single, multi-channel CVD graphene G-FET. The channel dimensions of the G-FET are designed to be $0.5 \mu\text{m} \times 80 \mu\text{m}$. The mixer circuit was designed in coplanar waveguide (CPW) technology due to its better performance at high frequency compared to microstrip [16] and was realized on a $100 \mu\text{m}$ thinned high resistive silicon substrate. The implementation uses a single G-FET and no balun is required, which makes the circuit

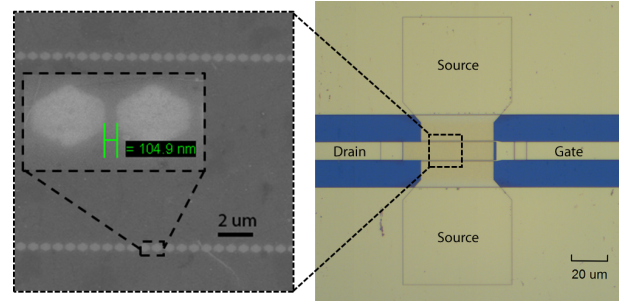


Fig. 1. Left is SEM image of patterned graphene channels and the right is close-up image of the two-finger G-FET.

topology more compact. Harmonic balance [17] and full wave EM simulation are applied for design and optimization of device and circuit, respectively. The measured CL is $34 \pm 3 \text{ dB}$ at 190-210 GHz with a minimum of 31.5 dB at 190 GHz. Albeit the performance of our proof-of-concept G-FET mixer on Si is inferior to CMOS [18], by transferring the process graphene has clear advantages for flexible electronics [19].

II. MIXER DESIGN AND FABRICATION

A. G-FET Design and Fabrication

In a resistive mixer, the drain-source channel is swept by a local oscillator (LO) on the gate as a time-varying resistor, $R_{ds}(t)$, which contains different harmonic frequency components. The unique p-n channel duality of graphene, which gives a highly symmetrical transfer characteristic, is essential for mixing at the second harmonic of the LO. According to [20], at low RF frequency the conversion loss is determined by $CL \propto 1/(\Gamma_{max} - \Gamma_{min})^2$. In order to get lower CL, higher Γ_{max} as well as lower Γ_{min} are required, which translates to $R_{max} \gg Z_0$ and $R_{min} \ll Z_0$. This requires G-FET components with high current on-off ratio and preferably with impedance level $Z_0 = \sqrt{R_{max}R_{min}} \approx 50 \Omega$.

Special care must be taken in designing G-FETs for resistive mixers, due to the lack of bandgap in graphene. The drain-source resistance is $R_{ds} = R_{channel} + R_c$. Here, $R_{channel}$ is the gate variable G-FET channel resistance which is essentially proportional to $L_{channel}/W_{channel}$, and R_c is the contact resistance at the graphene-metal interface which scales with the gate width, W_{gate} [21]. For the purpose of getting a lower R_{min} , a wide device is necessary. This simultaneously reduces R_{max} as G-FETs have no off-state. However, the gate capacitance limiting the high frequency mixer performance is determined by channel area, i.e. $L_{channel} \times W_{channel}$. In a normal G-FET channel structure, $L_{channel} = L_{gate}$ and

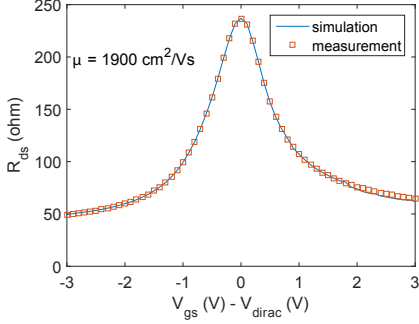


Fig. 2. Drain resistance R_{ds} versus gate bias voltage V_{gs} at $V_{ds} = 0.1$ V.

$W_{channel} = W_{gate}$, which limits the degrees of freedom in device design. A partial remedy was demonstrated in [22] and utilized in the mixer in [10]. Arrays of nanoconstrictions, i.e., bow-tie structured G-FET channels with $W_{gate} > W_{channel}$, are used to achieve higher current on-off ratio and proper impedance level. To optimize the device dimensions in the trade-off between impedance level and gate capacitance for CL at 200 GHz, the large-signal G-FET model proposed in [23] was set up in a standard circuit simulator (Agilent, ADS).

To fabricate the G-FET, a graphene sample was produced by chemical vapor deposition (CVD) process on copper film and transferred on a high resistive silicon substrate (10 kOhm bulk resistivity) covered by 90 nm SiO_2 . For the fabrication procedure, e-beam lithography, metalization by e-gun evaporation, lift-off steps and an initial oxygen plasma etching step (at 50-mTorr pressure) are applied to define mesas and for the sake of patterning the channel structure. Fig. 1 demonstrates the final dimensions of the G-FET channel optimized for lowest CL at $f_{RF} = 200$ GHz and shows the image of G-FET device. The component has a gate length of $0.5 \mu\text{m}$, where the gate-drain and the gate-source gaps are $0.1 \mu\text{m}$. Gate width is set to be $80 \mu\text{m}$ ($2 \times 40 \mu\text{m}$) and optimal channel width is given by $12 \mu\text{m}$, i.e. ~ 120 constrictions each of width ~ 100 nm. Fig. 2 shows the resulting transfer characteristics, R_{ds} versus V_{gs} , from simulation and measurement respectively. As can be seen, a current on-off ratio ~ 5 is achieved with $L_{gate} = 0.5 \mu\text{m}$.

B. Circuit Design and Fabrication

The subharmonic resistive G-FET mixer circuit was designed with a center frequency of $f_{RF} = 200$ GHz to downconvert to an $f_{IF} = 1$ GHz. The corresponding LO frequency is centered around 150.5 GHz. The circuit was realized in coplanar waveguide technology. If properly designed, relatively lower risk of parasitic mode propagation as well as lower dispersion for a given substrate thickness [16] make CPW competitive to microstrip in millimeter wave circuit applications. Nevertheless, due to substrate mode propagation and radiation loss at high frequency range, circuit substrate need to be sufficiently thin. To ensure suppression of such effects and for layout dimensional optimization, full wave EM simulations (CST microwave studio, FDTD) are applied. The

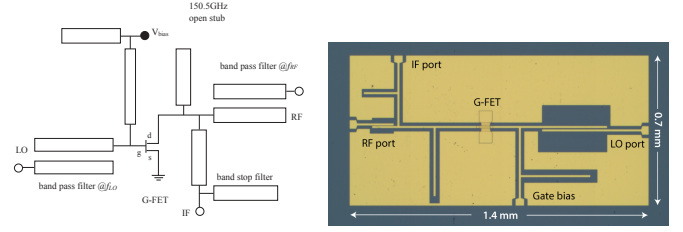


Fig. 3. a) The mixer topology and b) micrograph of the fabricated circuit.

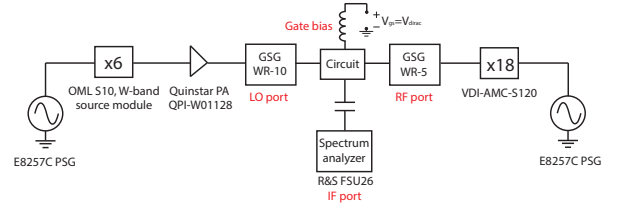


Fig. 4. Schematic block diagram of the measurement setup.

circuit topology of the proposed mixer is shown in Fig. 3a). The IF signal readout is through a bandstop filter which consist of a quarter wavelength open stub and a quarter wavelength transmission line at RF frequency. Coupled line bandpass filters are utilized both at the LO port branch and the RF port branch in order to block the DC gate bias and the IF signal, respectively. The G-FET requires a bias of $V_{gs} = V_{dirac}$ for optimum subharmonic mixing performance. Instead of applying high order coupled line filters, since $f_{LO} \approx f_{RF}/2$, single order filters are preferred due to the requirement of circuit simplification and area limitation. However, because of the narrowband characteristics of the stub filter and the broadband property of the simple coupled line filter, neither IF- nor RF-filters are capable of completely attenuating the LO signal. Therefore an additional bandstop filter at the LO frequency can be added on the drain side to improve both the LO-RF and LO-IF rejection capability.

The circuit layer was overlaid to the G-FET by e-beam lithography and e-gun evaporation of Ti (20 nm)/Au (500 nm). Finally, the silicon substrate was thinned down from $280 \mu\text{m}$ to $100 \mu\text{m}$ by a lapping process. Fig. 3b) displays the mixer on-chip layout, with chip measure $0.7 \times 1.4 \text{ mm}^2$.

III. MIXER CHARACTERIZATION

A. Measurement Setup

The fabricated circuit was characterized on-wafer using waveguide interfaced GSG microprobes, as sketched in Fig. 4. The LO chain consists of an OML $\times 6$ multiplied source followed by a W-band power amplifier. The RF power level is swept electronically and provided by a standard VDI-AMC-S120 $\times 18$ multiplier module. The LO and RF powers are calibrated using an Agilent E4419B power meter together with a W8486A power sensor and an Erickson PM4 power meter, respectively. The IF signal power is monitored on a FSU26 spectrum analyzer.

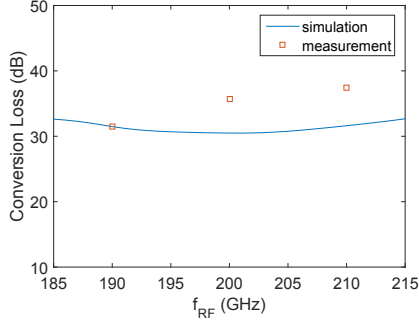


Fig. 5. Conversion loss vs. f_{RF} at $P_{LO} = 10$ dBm, $f_{IF} = 1$ GHz.

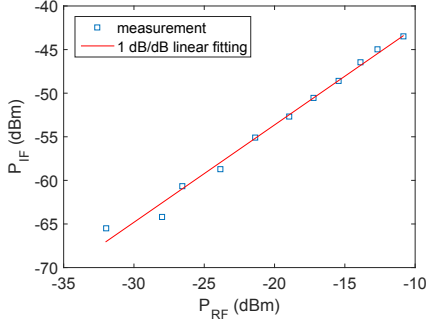


Fig. 6. P_{IF} vs. P_{RF} at $f_{RF} = 190$ GHz, $V_{gs} = V_{dirac}$ and $P_{LO} = 10$ dBm.

B. Results

The subharmonic mixer was biased at Dirac point $V_{gs} = V_{dirac}$. The conversion loss was measured to be 34 ± 3 dB over the frequency range from 190 GHz to 210 GHz with 10 dBm LO power and the overall minimum CL is 31.5 dB at 190 GHz, Fig. 5. The center frequency appears shifted to lower frequency, possibly due to tolerances in the circuit dimensions and substrate thickness. The measured IF output power for different RF input powers depicted in Fig. 6 confirms the linear operation regime of the mixer.

Fig. 7 demonstrates the conversion loss versus gate bias voltage at 200 GHz RF frequency. Due to the utilization of symmetrical transfer characteristic of G-FET, mixer performance is strongly dependent on DC gate bias point and the CL increases 6 dB when deviating ± 1 V from V_{dirac} . Because of the instability of G-FET, the V_{dirac} might have drifted ± 0.4 V during measurements which could give ± 2 dB variation.

IV. CONCLUSION

In this paper, a 200 GHz integrated subharmonic resistive mixer based on a G-FET is reported. The mixer is realized in CPW technology on a $100 \mu\text{m}$ high resistive silicon substrate. An array of bow-tie structured graphene is applied in the G-FET channel in order to obtain simultaneously a more suitable impedance level as well as higher current on-off ratio. Conversion loss over the RF frequencies from 190 to 210 GHz is measured to be $34 \text{ dB} \pm 3 \text{ dB}$ and overall

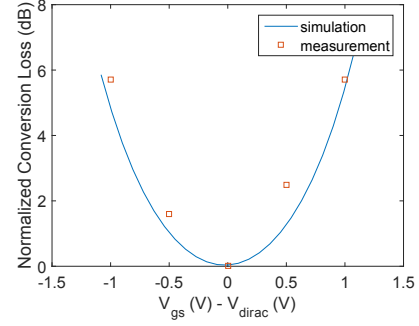


Fig. 7. Conversion loss vs. V_{gs} at $P_{LO} = 10$ dBm and $f_{RF} = 200$ GHz.

TABLE I
COMPARISON OF GRAPHENE-BASED RESISTIVE MIXERS

| | [13] | [14] | [15] | [10] | [24] | This work |
|----------------------|------|------|------|------|------|-----------|
| RF frequency (GHz) | 2 | 3.6 | 5 | 27 | 330 | 190 |
| Conversion Loss (dB) | 14 | 33 | 20 | 18 | 65 | 31.5 |
| Subharmonic Order | 1 | 1 | 2 | 2 | 6 | 2 |

minimum CL is 31.5 dB at 190 GHz and 10 dBm LO power. The mixer performance comparison among this work and previous graphene-based implementations are presented in Table I. As can be seen, our results represent a 7-fold improvement in operating frequency compared to previously reported G-FET integrated circuits and a significant (>30 dB) performance improvement to existing graphene based mixer in this frequency range [24]. This demonstrates the potential applicability of graphene in ubiquitous millimeter wave and even terahertz wave receivers.

ACKNOWLEDGMENT

This research was supported financially by the Swedish Foundation of Strategic Research (SSF).

REFERENCES

- [1] K. S. Novoselov, A. K. Geim, S. V. Morozov, D. Jiang, Y. Zhang, S. V. Dubonos, I. V. Grigorieva, and A. A. Firsov, "Electric field effect in atomically thin carbon films," *Science*, vol. 306, no. 5659, pp. 666-669, Oct. 2004.
- [2] F. Schwierz, "Graphene Transistors: Status, Prospects, and Problems," *Proc. IEEE*, vol. 101, no. 7, pp. 1567-1584, Jun. 2013.
- [3] J. Wells, "Faster than fiber: The future of multi-Gbps wireless," *IEEE Microw. Mag.*, vol. 10, no. 3, pp. 104-112, May 2009.
- [4] R. Appleby and H. B. Wallace, "Standoff detection of weapons and contraband in the 100 GHz to 1 THz region," *IEEE Trans. Antennas Propag.*, vol. 55, no. 11, pp. 2944-2956, Nov. 2007.
- [5] O. Habibpour, Z. S. He, W. Strupinski, N. Rorsman, T. Ciuk, P. Ciepielewski, and H. Zirath, "Graphene FET Gigabit On-Off Keying Demodulator at 96 GHz," *IEEE Electron Device Lett.*, vol. 37, no. 3, pp. 333-336, Mar. 2016.
- [6] J. S. Moon, H.-C. Seo, M. Antcliffe, S. Lin, C. McGuire, D. Le, L. O. Nyakiti, D. K. Gaskill, P. M. Campbell, K.-M. Lee, and P. Asbeck, "Graphene FET-Based Zero-Bias RF to Millimeter-Wave Detection," *IEEE Electron Device Lett.*, vol. 33, no. 10, pp. 1357-1359, Oct. 2012.
- [7] L. Vicarelli, M. S. Vitiello, D. Coquillat, A. Lombardo, A. C. Ferrari, W. Knap, M. Polini, V. Pellegrini, and A. Tredicucci, "Graphene field-effect transistors as room-temperature terahertz detectors," *Nat. Mater.*, vol. 11, pp. 865-871, Sep. 2012.

- [8] A. Zak, M. A. Andersson, M. Bauer, J. Matukas, A. Lisauskas, H. G. Roskos, and J. Stake "Antenna-Integrated 0.6 THz FET Direct Detectors Based on CVD Graphene," *Nano Lett.*, vol. 14, no. 10, pp. 5834-5838, Sep. 2014.
- [9] S.-J. Han, A. Valdes Garcia, S. Oida, K. A. Jenkins, and W. Haensch, "Graphene radio frequency receiver integrated circuit," *Nat. Commun.*, vol. 5, pp. 3086-1-3086-6, Jan. 2014.
- [10] O. Habibpour, J. Vukusic, and J. Stake, "A 30-GHz Integrated Subharmonic Mixer Based on a Multichannel Graphene FET," *IEEE Trans. Microw. Theory Techn.*, vol. 61, no. 2, pp. 841-847, Feb. 2013.
- [11] M. Tanzid, M. A. Andersson, J. Sun, and J. Stake, "Microwave noise characterization of graphene field effect transistors," *Appl. Phys. Lett.*, vol. 104, no. 1, pp. 013502, Feb. 2014.
- [12] Z. Guo, R. Dong, P. S. Chakraborty, N. Lourenco, J. Palmer, Y. Hu, M. Ruan, J. Hankinson, J. Kunc, J. D. Cressler, C. Berger, and W. A. de Heer, "Record Maximum Oscillation Frequency in C-Face Epitaxial Graphene Transistors," *Nano Lett.*, vol. 13, no. 3, pp. 942-947, Feb. 2013.
- [13] J. S. Moon, H.-C. Seo, M. Antcliff, D. Le, C. McGuire, A. Schmitz, L. O. Nyakiti, D. K. Gaskill, P. M. Campbell, K.-M. Lee, and P. Asbeck, "Graphene FETs for Zero-Bias Linear Resistive FET Mixers," *IEEE Electron Device Lett.*, vol. 34, no. 3, pp. 464-467, Feb. 2013.
- [14] H. Lyu, H. Wu, J. Liu, Q. Lu, J. Zhang, X. Wu, J. Li, T. Ma, J. Niu, W. Ren, H. Cheng, Z. Yu, and H. Qian, "Double-Balanced Graphene Integrated Mixer with Outstanding Linearity," *Nano Lett.*, vol. 15, no. 10, pp. 6677-6682, Sep. 2015.
- [15] M. A. Andersson, O. Habibpour, J. Vukusic and J. Stake, "Resistive Graphene FET Subharmonic Mixers: Noise and Linearity Assessment," *IEEE Trans. Microw. Theory Techn.*, vol. 60, no. 12, pp. 4035-4042, Dec. 2012.
- [16] F. Schnieder, T. Tischler, and W. Heinrich, "Modeling dispersion and radiation characteristics of conductor-backed CPW with finite ground width," *IEEE Trans. Microw. Theory Techn.*, vol. 57, no. 1, pp. 137-143, Jan. 2003.
- [17] S. A. Maas, *Nonlinear Microwave and RF Circuits*, Artech House, 2003.
- [18] B. Khamaisi, and E. Socher, "130-320-GHz CMOS Harmonic Down-Converters Around and Above the Cutoff Frequency," *IEEE Trans. Microw. Theory Techn.*, vol. 63, no. 7, pp. 2275-2288, Jul. 2015.
- [19] N. Petrone, I. Meric, T. Chari, K. L. Shepard, and J. Hone, "Graphene Field-Effect Transistors for Radio-Frequency Flexible Electronics," *IEEE J. Electron Devices Soc.*, vol. 3, no. 1, pp. 44-48, Jan. 2015.
- [20] K. Yhland, "Simplified analysis of resistive mixers," *IEEE Microw. Wireless Compon. Lett.*, vol. 17, no. 8, pp. 604-606, Aug. 2007.
- [21] J. T. Smith, A. D. Franklin, D. B. Farmer, and C. D. Dimitrakopoulos, "Reducing contact resistance in graphene devices through contact area patterning," *ACS Nano*, vol. 7, no. 4, pp. 3661-3667, Mar. 2013.
- [22] Y. Lu, B. Goldsmith, D. R. Strachan, J. H. Lim, Z. Luo, and A. T. Charlie Johnson, "High-on/off-ratio graphene nanoconstriction field effect transistor," *Small*, vol. 6, no. 23, pp. 2748-2754, Oct. 2010.
- [23] O. Habibpour, J. Vukusic, and J. Stake, "A Large-Signal Graphene FET Model," *IEEE Trans. Electron Devices.*, vol. 59, no. 4, pp. 968-975, Apr. 2012.
- [24] C. Vazquez Antuna, A. I. Hadarig, S. Ver Hoeye, M. Fernandez Garcia, R. Cambolor Diaz, G. R. Hotopan, F. Las Heras Andres, "High-Order Subharmonic Millimeter-Wave Mixer Based on Few-Layer Graphene," *IEEE Trans. Microw. Theory Techn.*, vol. 63, no. 4, pp. 1361-1369, Apr. 2015.